CrystEngComm

Accepted Manuscript

ROYAL SOCIETY OF CHEMISTRY

www.rsc.org/crystengcomm

CrystEngComm

RSCPublishing

ARTICLE

Solvent-assisted Construction of Diverse Mg-TDC Coordination Polymers

Cite this: DOI: 10.1039/x0xx00000x

Ying Song,[ab] Mei-Ling Feng,[a] Zhao-Feng Wu[ab] and Xiao-Ying Huang*[a]

Received 00th January 2012,
Accepted 00th January 2012

DOI: 10.1039/x0xx00000x

www.rsc.org/

Upon alteration of selected solvents, the reactions of 2,5-thiophenedicarboxylic acid (H_2TDC) and $Mg(NO_3)_2{\cdot}6H_2O$ afforded four diverse coordination polymers, namely $Mg_2(TDC)_2(EG)_{2.5}{\cdot}0.5EG$ (**1**), Mg(TDC)(DMSO) (**2**), $(Me_2NH_2)[(Mg_2(TDC)_2(Ac)]{\cdot}1.5DMA{\cdot}0.5H_2O$ (**3**), and $[Mg_2(TDC)_2(DMF)_2(EtOH)(H_2O)_2]{\cdot}DMF$ (**4**) (EG = ethylene glycol, DMSO = dimethyl sulfoxide, Ac = acetate anion, DMA = N, N'-dimethyl-acetamide, DMF = N, N'-dimethyl-formamide, EtOH = ethanol). Single-crystal X-ray diffraction analyses indicated that compounds **1-3** possessed a three-dimensional (3D) network while **4** adopted a two-dimensional (2D) layered structure. Noticeably, the coordinated solvent molecules adopt distinct coordination modes which play a vital role in constructing the Mg-TDC structures. In **1**, the solvent EG molecules as bi-dentate bridging ligand help interconnecting the Mg-TDC layers to a 3D framework. Whereas the solvent DMSO molecules in **2** and the Ac^- anions generated from decomposition of DMA in **3** are coordinated in a μ_2-fashion and (k^2-k^2)-μ_3 mode, respectively, leading to infinite chains as secondary building units. In the layered structure of **4**, the collaboration of coordinated DMF, EtOH and H_2O molecules assists in inducing the noncentrosymmetric structure. The compounds were fully characterized by PXRD, TGA, EA, IR and the luminescent properties of **1-3** and the second-harmonic generation (SHG) property of **4** were studied. **3** emitted bright green light upon the excitation of 365 nm UV light. While **4** displayed sound SHG response.

Introduction

The modular nature and crystallinity of coordination polymers (CPs) facilitate the research of their structures at a molecular level.[1] Due to the wide choice of metal nodes and organic linkers, various CPs with diverse structures and properties have been synthesized and investigated.[2] The majority of CPs is focused on those based on the d-block, p-block and rare earth metal ions, whereas the CPs based on s-block metal ions such as Mg^{2+} were less explored.[3] In fact, the Mg^{2+} has many outstanding merits for constructing CPs; for instance, it has light molecular mass and diverse coordination modes, and it is eco-friendly and abundant in the earth's crust. Recently, the Mg-CPs have shown some excellent properties that are superior to those of the CPs based on other metal ions;[4] for example, a Mg_2(DOT) (DOT = 2,5-dioxidoterephthalate) CP shows excellent CO_2 adsorption capacity outperforming its isomers based on Zn(II), Co(II) and Ni(II) ions,[4a] and it can sufficiently capture CO_2 from CH_4 which is essential for natural gas purification.[4b]

The solvent used in the synthesis of CPs is a crucial parameter which governs reaction kinetics and thermodynamics during the coordination process.[5] The solvent molecule can act as a guest being encapsulated in structural lattice to affect the structural construction indirectly,[6] or as a ligand that has a significant impact on secondary building unit (SBU) assembly and even on structural dimensionality[7] and framework topology.[8] In addition, some acyl-amide solvents such as DMF, DMA and DEF (N, N'-diethyl-formamide) may undergo in-situ decomposition during the reaction process to produce small ions which may also serve as a coordinated ligand and/or charge-compensating agent in the resulting structure.[9] Though the Mg(II) ion has similar coordination nature with first-row transition metal ions such as Co(II) and Zn(II), its coordination bonds are of relatively more ionic nature.[3b] Indeed, the Mg(II) ion is easily coordinated by polar solvent molecules with oxygen donors. As a result, the variation of solvent molecules may exert a significant effect on the formation of different Mg-CPs.[3b, 10]

In this work, we attempted to exploit the different roles of solvent molecules in the construction of Mg-CPs. By reacting $Mg(NO_3)_2{\cdot}6H_2O$ with 2,5-thiophenedicarboxylic acid (H_2TDC) in the selected solvents, we isolated four Mg-TDC CPs with varied structures, namely $Mg_2(TDC)_2(EG)_{2.5}{\cdot}0.5EG$ (**1**), Mg(TDC)(DMSO) (**2**), $(Me_2NH_2)[(Mg_2(TDC)_2(Ac)]{\cdot}1.5DMA{\cdot}0.5H_2O$ (**3**), and

$[Mg_2(TDC)_2(DMF)_2(EtOH)(H_2O)_2]\cdot DMF$ (**4**) (EG = ethylene glycol, DMSO = dimethyl sulfoxide, Ac = acetate anion, DMA = N, N'-dimethyl-acetamide, DMF = N, N'-dimethyl-formamide, EtOH = ethanol). In **1**, the bi-dentate EG molecule as a bridging ligand participates in interlinking the Mg-TDC layers to three-dimensional (3D) framework, whereas the μ_2-DMSO molecule in **2** and the Ac^- anion with a $(k^2\text{-}k^2)\text{-}\mu_3$ fashion in **3** contribute to constructing the one-dimensional (1D) chain-like SBUs of the structures; finally the coexistence of multiple coordinated solvent molecules including DMF, EtOH and H_2O brings about symmetry-breaking, leading to the noncentrosymmetric (NCS) structure of **4** with sound SHG response.

Experimental

Materials and physical measurements

All analytical grade chemicals employed in this study were commercially available and used without further purification. Powder X-ray diffraction (PXRD) patterns were recorded in the angular range of 2θ = 3-65 ° on a Miniflex II diffractometer using Cu$K\alpha$ radiation. Thermogravimetric analyses were carried out with a NETZSCH STA 449F3 unit at a heating rate of 10 ˚C /min under a nitrogen atmosphere. The TG-MS was carried out on a STA449C-QMS403C. Elemental analyses (EA) for C, H, N were performed on a German Elementary Vario EL III instrument. Fourier transform infrared (FT-IR) spectra were taken on a Nicolet Magna 750 FT-IR spectrometer in the 4000–400 cm^{-1} region by using KBr pellets. The fluorescence spectra were recorded using an Edinburgh FLS920 fluorescence spectrophotometer at room temperature. The powder Second-Harmonic Generation (SHG) response was measured on polycrystalline samples by using the experimental method adapted from that reported by Kurtz and Perry.[11] 1064 nm radiation generated by a Q-switched Nd:YAG solid-state laser was used as the fundamental frequency light. The sample was ground and then pressed into a disk with diameter of 8 mm which was then put between glass microscope slides and secured with tape in a 1 mm thick aluminum holder. The second harmonic signals were compared with that of standard nonlinear optical material potassium dihydrogen phosphate (KDP = KH_2PO_4) to determine the relative SHG efficiency of **4**.

Syntheses of compounds 1-4

All the four compounds were synthesized by solvothermal methods. The reaction conditions for obtaining compounds **1**, **2** and **3** are similar to each other with alteration of the solvents used. Typically, a mixture of $Mg(NO_3)_2\cdot 6H_2O$, 2,5-thiophenedicarboxylic acid and solvent was sealed in a stainless steel reactor with a 20 (or 28) mL Teflon liner and heated in the oven at 150 ˚C for 3 days, followed by cooling to room temperature. The resulting crystals of **1-4** were selected by hand and washed with anhydrous ethanol followed by drying in the air. The yields were calculated based on $Mg(NO_3)_2\cdot 6H_2O$.

$Mg_2(TDC)_2(EG)_{2.5}\cdot 0.5EG$ (1). The reaction of a mixture of 0.251 g $Mg(NO_3)_2\cdot 6H_2O$, 0.257 g 2,5-thiophenedicarboxylic acid, 3 mL ethylene glycol and 3 mL methyl cyanide resulted in brown bipyramidal crystals; yield 0.135 g, 46%. Elemental analysis (%): calc. for $C_{18}H_{22}O_{14}S_2Mg_2$: C, 37.59%; H, 3.86%; Found: C, 36.99%; H, 3.90%.

Mg(TDC)(DMSO) (2). The reaction of a mixture of 0.261 g $Mg(NO_3)_2\cdot 6H_2O$, 0.174 g 2,5-thiophenedicarboxylic acid, 4 mL dimethyl sulfoxide and 2 mL methanol resulted in colorless block-like crystals; yield 0.150 g, 55%. Elemental analysis (%): calc. for $C_8H_8O_5S_2Mg$: C, 35.25%; H, 2.96%; Found: C, 35.09%; H, 3.15%.

$(Me_2NH_2)[(Mg_2(TDC)_2(Ac)]\cdot 1.5DMA\cdot 0.5H_2O$ (3). A mixture of 0.101 g $Mg(NO_3)_2\cdot 6H_2O$, 0.067 g 2,5-thiophenedicarboxylic acid and 4 mL N, N'-dimethylacetamide was heated at 150 ˚C for 3 days follow by programmed cooling in a rate of 0.67 ˚C/min to 30 ˚C. Light-yellow quadrangular crystals were resulted in; yield 0.210 g, 42%. Elemental analysis (%): calc. For $C_{22}H_{29.5}N_{2.5}O_{12}S_2Mg_2$: C, 41.69%; H, 4.69%; N, 5.52%; Found: C, 41.63%; H, 5.25%; N, 6.03%.

$[Mg_2(TDC)_2(DMF)_2(EtOH)(H_2O)_2]\cdot DMF$ (4). A mixture of 0.252 g $Mg(NO_3)_2\cdot 6H_2O$, 0.174 g 2,5-thiophenedicarboxylic acid, 5 mL N, N'-dimethylformamide, 1 mL ethanol, 0.5 mL distilled water was heated at 100 ˚C for 3.5 days followed by a programmed cooling at a rate of 0.39 ˚C/min to 30 ˚C. Colorless block-like crystals were obtained; yield 0.180 g, 52%. Elemental analysis (%): calc. for $C_{23}H_{34}N_3O_{14}S_2Mg_2$: C, 40.08%; H, 4.97%; N, 6.10%; Found: C, 39.33%; H, 4.89%; N, 6.11%.

Fig. 1 Photographs of crystals of **1-4** under an optical microscope.

Single–crystal structure determination

Suitable single crystals of compounds **1-4** were carefully selected under an optical microscope and glued to thin glass fibres. The photographs of selected crystals for compounds **1-4**

are illustrated in Fig. 1. Data collections were performed on an Oxford Xcalibur Eos diffractometer with graphite-monochromated Mo$K\alpha$ radiation (λ = 0.71073 Å) for **1** and **4** at room temperature and on a SuperNova CCD diffractometer with graphite-monochromated Cu$K\alpha$ radiation (λ = 1.5418 Å) for **2** and **3** at 100 K, respectively. The structures were solved by direct methods and refined by full-matrix least-squares on F^2 by using the program package SHELX-97.[12] All non-hydrogen atoms were refined anisotropically. The positions of hydrogen atoms were generated geometrically with assigned isotropic thermal parameters, and allowed to ride on their respective parent atoms before the final cycles of least–squares refinements. In **1**, the C and H atoms on the half bridging EG molecule and one of the terminal EG molecules were disordered over two positions with refined S.O.F. ratios of 0.787(16)/0.213(16) and 0.537(9)/0.463(9), respectively. Whereas in **2**, the S, C and H atoms of the four unique DMSO molecules were all disordered over two positions with refined S.O.F. ratios of 0.866(4)/0.134(4), 0.737(5)/0.263(5), 0.867(4)/0.133(4) and 0.766(5)/0.234(5), respectively. For compound **3**, the guest solvent molecules and cations were highly disordered, thus the PLATON/SQUEEZE[13] was employed to calculate the contributions to the diffraction from the solvent region and thereby produced a set of solvent-free diffraction intensities. The final formula of **3** was calculated from the SQUEEZE results combined with elemental analysis data and TGA-MS data (Fig. S1). In **4** the terminal DMF molecule was disordered over two positions with refined S.O.F. ratio of 0.659(9)/0.341(9), and the half of free DMF molecule was disordered with S.O.F. of 0.5 (the O9 atom rides on a mirror plane). The soft restraints of DFIX, SIMU, SADI, ISOR, DELU were applied on the disordered atoms to keep their geometries and atomic displacement parameters reasonable. The empirical formulae of **1**, **2**, and **4** were confirmed by the thermo-gravimetric analyses (TGA) and element analyses (EA) results. Details of crystallographic data and structural refinement parameters are summarized in Table 1. CCDC nos. 1032293 (**1**), 1032294 (**2**), 1032295 (**3**) and 1032296 (**4**) contain the supplementary crystallographic data for this paper.

Table 1 Crystallographic data for **1-4**.

	1	**2**	**3**	**4**
Empirical formula	$C_{18}H_{22}Mg_2O_{14}S_2$	$C_{32}H_{32}Mg_4O_{20}S_8$	$C_{22}H_{29.5}Mg_2N_{2.5}O_{12}S_2$	$C_{23}H_{34}Mg_2N_3O_{14}S_2$
Formula Mass	575.10	1090.30	633.72	689.27
Crystal system	triclinic	triclinic	tetragonal	monoclinic
Space group	*P*-1	*P*-1	$P4_2/nmc$	*Cm*
a/Å	9.6484(6)	10.6233(3)	22.2398(1)	12.9363(6)
b/Å	11.7939(7)	14.7624(5)	22.2398(1)	15.8580(8)
c/Å	11.8603(5)	15.8152(4)	12.3010(1)	9.0474(7)
α/ °	73.671(4)	76.453(2)	90.00	90
β/ °	67.426(5)	74.011(2)	90.00	120.978(10)
γ/ °	74.356(5)	70.088(3)	90.00	90
V/Å^3	1175.85(11)	2214.52(11)	6084.18(6)	1591.28(16)
Z	2	2	8	2
T/K	293(2)	100(2)	100(2)	293(2)
Flack parameter	/	/	/	-0.07(12)
F(000)	596	1120	2648	722
ρ_{calcd}/g cm^{-3}	1.624	1.635	1.384	1.439
μ/mm^{-1}	0.352	4.983	2.530	0.276
Measured refls.	9808	23275	17000	3600
Independent refls.	4806	9212	3179	2569
No. of parameters	357	705	134	269
R_{int}	0.0269	0.0224	0.0228	0.0242
R_1 ($I > 2\sigma(I)$)[a]	0.0499	0.0626	0.0308	0.0443
$wR(F^2)$ ($I > 2\sigma(I)$)[b]	0.1238	0.1585	0.0898	0.1087
GOF	1.007	1.011	1.013	1.038

[a] $R_1 = \sum \| F_o | - | F_c \| / \sum | F_o |$. [b] $wR_2 = [\sum w(F_o^2 - F_c^2)^2 / \sum w(F_o^2)^2]^{1/2}$.

Results and discussion

Syntheses

The effects of temperature and solvents on the syntheses of four compounds have been explored. The various reactions for the preparation of compounds **1-4** are listed in Table S1. The experiments showed that compound **1** could be obtained at 150~160 ˚C in a mixed solvent of EG and acetonitrile. In addition to EG, an auxiliary solvent with low boiling point (such as acetonitrile, acetone and methanol) was indispensable to obtain the crystals of **1** which might help in decreasing the viscosity of the reaction solution. While **2** could be isolated at 140~150 ˚C in a mixed solvent of DMSO and methanol; at a higher temperature of 170 ˚C, the DMSO decomposed and the crystals of $MgSO_4$ were identified. Noticeably, at 150 ˚C **2** could always be obtained in DMSO no matter whether the auxiliary solvent was presented or not. The auxiliary solvents could be polar ones such as DMF, ethanol, acetonitrile, and nonpolar ones such as benzene. However, it was evident that the presence of auxiliary solvents such as methanol can help increasing the yield of **2** greatly. To our knowledge, the acetamide-type solvents like DMF and DMA may decompose to produce $HCOO^-$ (CH_3COO^-) and $[Me_2NH_2]^+$ with or without

the existence of H_2O above a specific temperature (about 100 ˚C or higher) under solvothermal conditions and this was further confirmed by the syntheses of **3** and **4**. **3** could be obtained in DMA at 120 ~ 150 ˚C; at 150 ˚C the presence of a micro amount of H_2O and methanol did not affect the formation of **3**. As for **4**, it could be obtained at 100 ˚C in a mixed solvent of DMF, ethanol and H_2O, but when the temperature was increased to 120 ˚C and above the DMF decomposed and a well-known Mg-formate, namely $(Me_2NH_2)[Mg(HCOO)_3]$ was obtained.[14] Since the H_2O existed in **4**, our experiments showed that crystals of **4** could not be isolated without water in the solvent system.

Crystal structure descriptions

$Mg_2(TDC)_2(EG)_{2.5}$·0.5EG (1). Compound **1** belongs to the *P*-1 space group. The structure features a 3D framework constructed by bridging solvent EG molecules and two-connected Mg^{2+} nodes interconnecting Mg-TDC layers, Fig. 2. The asymmetric unit contains one formula unit, including one and two halves of Mg^{2+} ions (each located in an inversion center), two TDC^{2-} ligands, two terminal coordinated EG molecules, half of an EG molecule as bridging ligand and half of a free EG molecule (each with an inversion center passing through the middle of C-C bond). All the Mg^{2+} ions adopt octahedral geometry, Fig. S2a. The Mg1 located in an inversion center is coordinated by six oxygen atoms from six TDC^{2-} ligands. Whereas the coordination sphere of Mg2 includes five oxygen donors from four TDC^{2-} ligands and one oxygen atom from an EG molecule that acts as a bridging ligand linking to another Mg2 ion. The Mg3 also lies in an inversion center; its coordination mode is quite special in that it is surrounded by two oxygen atoms from two TDC^{2-} ligands in the apical positions and four oxygen atoms from four terminal EG molecules in the equatorial plane. Thus, the Mg3 actually can be regarded as a two-connected node, Fig. S3a. The four distinct EG molecules existing in the structure can be denoted as EG1, EG2, EG3 and EG4, corresponding to the EG molecules that act as bridging ligands (EG1), terminal ligands (EG2 and EG3) and free guest molecules (EG4), Fig. S4.

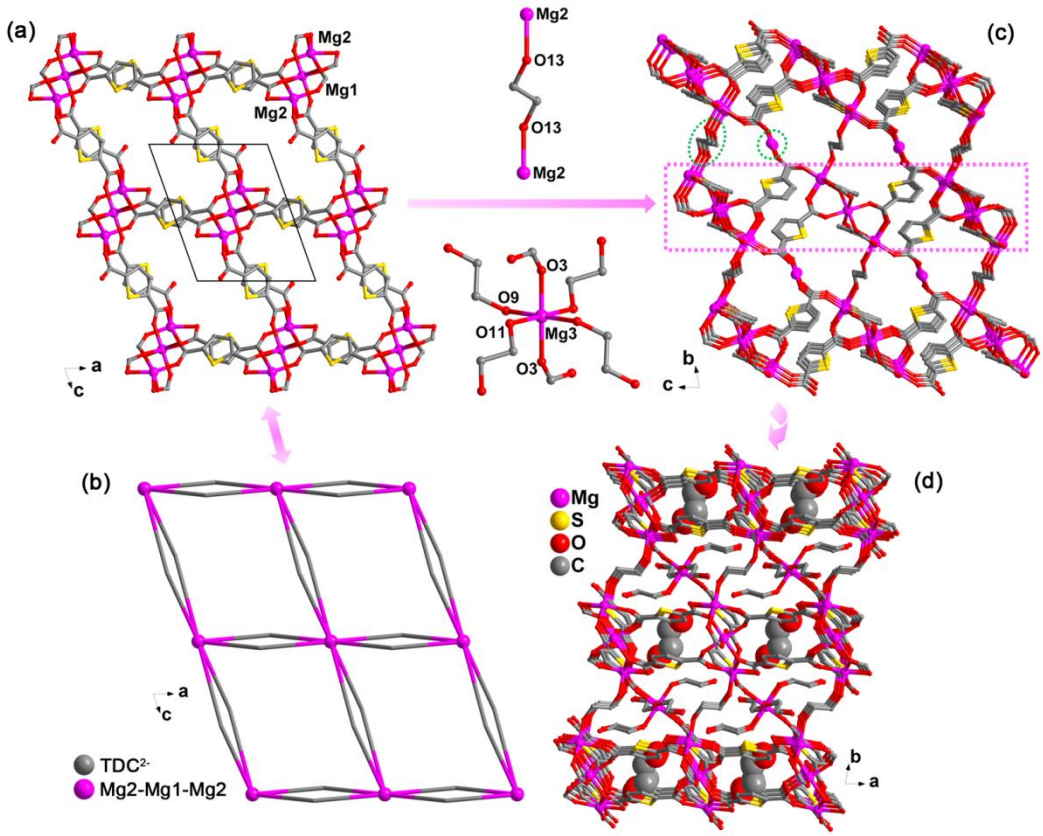

Fig. 2 (a) View of a Mg-TDC layer in the *ac* plane fabricated by TDC^{2-} ligands interconnecting Mg2-Mg1-Mg2 clusters in **1**. (b) Simplified net of the layer in **1**. (c) View of the 3D structure along the *a* axis showing the linking roles of EG1 molecules and Mg3 nodes. The four terminal coordinated EG molecules of Mg3 are omitted for clarity. (d) View of the 3D structure of **1** along the *c* axis with free EG molecules located in the voids in a space-filling mode. All the H atoms are omitted for clarity.

There are two independent TDC^{2-} ligands denoted as L-I and L-II, respectively. The L-I connects to four Mg^{2+} ions (Mg1, Mg2, Mg2, Mg3) in a $(k^1\text{-}k^1\text{-}\mu_2)\text{-}(k^1\text{-}k^1\text{-}\mu_2)\text{-}\mu_4$ mode, whereas the L-II links to four Mg^{2+} ions (Mg1, Mg2, Mg1, Mg2) in a $(k^1\text{-}k^1\text{-}\mu_2)\text{-}(k^1\text{-}k^2\text{-}\mu_2)\text{-}\mu_4$ mode, Fig. S3b. As a result, a tri-nuclear $[Mg_3]$ unit is evident as SBU in a Mg2-Mg1-Mg2 sequence. Then each $[Mg_3]$ unit is interlinked to other four same $[Mg_3]$ units by TDC^{2-} ligands in a "double-bridge" mode to give rise to a 2D layer along the *ac* plane, Fig. 2a; the linking modes among the SBUs are further demonstrated as a simplified net in Fig. 2b.

Then, the adjacent layers are interlinked to a 3D framework by EG1 molecules that coordinate to two Mg2 ions from two adjacent layers and Mg3 ions that bind to two carboxylic O3 atoms of L-I from two adjacent layers, Fig. 2c. The EG2 and EG3 molecules are located in the inter-layered spaces and the EG4 molecules are filled in the voids along the *c* axis, Fig. 2d. Interestingly, the EG molecules play different roles simultaneously in constructing the structure of **1**, that is, as guest molecules (EG4), terminal ligands (EG2 and EG3), and bridging ligands (EG1). In the reported CPs, there are several examples in which the EG molecules act as bridging ligands in the structure where the roles of them can be sorted to two types: 1) to take part in forming SBUs, exemplified by the formation of 1D chains in $[Co_3(BDC)_3(EG)_4]$[15] and $\{Na_2NiPr(\mu_4\text{-}ClO_4)(\mu_2\text{-}EG))\text{-}(\mu_4\text{-}ptc)_2(H_2O)_8\}\cdot 4.5H_2O\}_n$;[16] 2) to help increasing structural dimensionality, exemplified by $\{[Mn(C_{14}H_6O_6S)(C_2H_6O_2)(H_2O)_2]\cdot C_4H_9NO\}_n$[17] in which the EG molecules interlink 1D Mn-L chains to 2D layers, and $[Cd(HBTC)(EG)\cdot 8(H_2O)]$[18] in which they act as pillars to link 2D layers of Cd-L to 3D framework. The latter is further illustrated in **1**.

Mg(TDC)(DMSO) (2). The structure of **2** belongs to the *P*-1 space group and features a 3D network constructed by TDC^{2-} ligands and DMSO molecules interlinking Mg^{2+} ions, Fig. 3. The asymmetric unit contains four formula units though the four independent Mg^{2+}, TDC^{2-} and DMSO all adopt similar coordination modes. This may probably be due to the difference in the disordering degree of DMSO molecules. The four unique Mg^{2+} ions are all six-coordinated (Fig. S2b) by four TDC^{2-} ligands in the equatorial plane and two DMSO molecules in the apical positions, which differ slightly in Mg-$O_{carboxylate}$ bond lengths and O-Mg-O angles from each other, Fig. S5a. While the four unique TDC^{2-} ligands all adopt the common $(k^1\text{-}k^1\text{-}\mu_2)\text{-}(k^1\text{-}k^1\text{-}\mu_2)\text{-}\mu_4$ mode, Fig. S5b. Similarly, the four independent DMSO molecules all bind to two Mg^{2+} ions in a μ_2-fashion, Fig. 3a.

Along the *b* axis, adjacent Mg^{2+} ions are interconnected by two $(COO)^-$ groups from TDC^{2-} ligands in a "bi-bridge" mode and one DMSO molecule in a μ_2-fashion, respectively, to form a 1D infinite chain, Fig. 3b. In the chain, the four unique Mg^{2+} ions are periodically ordered to form a Mg4-Mg3-Mg2-Mg1-Mg4-Mg3-Mg2-Mg1 array. Then, each chain is interlinked to other four chains by TDC^{2-} ligands to give rise to a 3D framework, in which the rhombic tunnels along the *b* axis are formed filled by the S, C, H atoms of the bridging DMSO molecules, Fig. 3c. Similarly, the DMSO molecules also act as bridging ligands in $[Mn(DTDC)(\mu_2\text{-}DMSO)]$[19] and

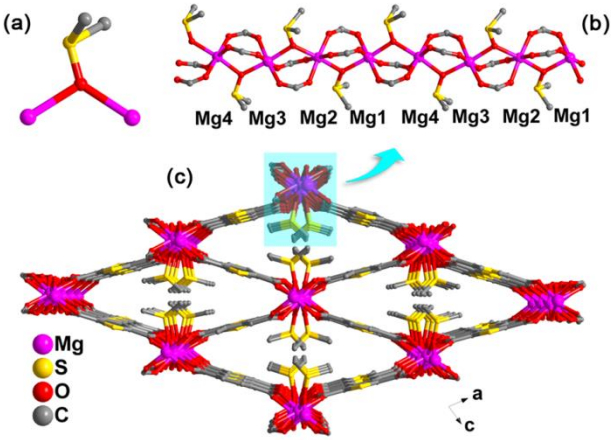

Fig. 3 (a) The linking mode of DMSO molecules with Mg^{2+} ions in **2**. (b) The $[Mg(COO)_2DMSO]_n$ infinite chain in **2**. (c) View of the 3D structure of **2**. All the H atoms are omitted for clarity.

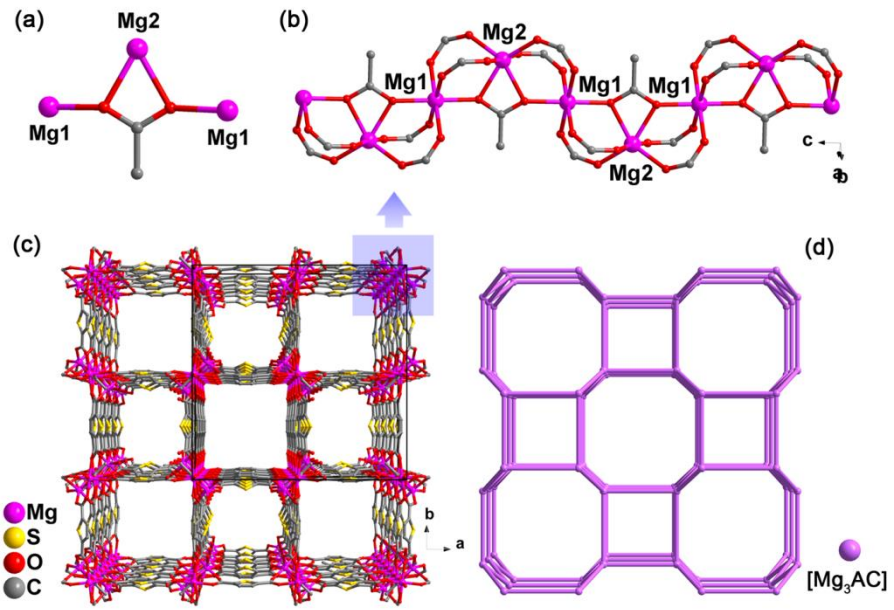

Fig. 4 (a) The linking mode of Ac^- anions with Mg^{2+} ions in **3**. (b) The Mg-COO-Ac chain in **3** showing the sequence of Mg^{2+} centers. (c) View of the 3D framework of **3** along the *c* axis. $[Me_2NH_2]^+$ cations, DMA and H_2O molecules in the channels are not shown for clarity. (d) The topology of **3**. All the H atoms are omitted for clarity.

[Pb(*p*-BDC)(μ_2-DMSO)].[20] For other solvent molecules playing the similar role, there is also a Mg-based CP, namely Mg(ndc)(μ_2-nmp)·0.5H_2O (nmp = 1-methyl-2-pyrrolidinone).[10]

$(Me_2NH_2)[(Mg_2(TDC)_2(Ac)]\cdot 1.5DMA\cdot 0.5H_2O$ (3). Compound **3** belongs to the $P4_2/nmc$ space group. It features a 3D anionic open framework fabricated by TDC^{2-} ligands and Ac^- anions linking Mg^{2+} ions, with $[Me_2NH_2]^+$ as counter ions located in the tunnels along the *c* axis, Fig. 4. Its asymmetric unit contains half of the formula unit including two halves of Mg^{2+} ions, two halves of TDC^{2-} ligands and half of Ac^- anion, each of which is located in an inversion center. Both the Mg^{2+} ions adopt an octahedral configuration, Fig. S2c. The Mg1 is coordinated by four TDC^{2-} ligands in the equatorial plane and two Ac^- anions in the apical positions, while the Mg2 is connected by four TDC^{2-} and one Ac^- anion in a chelating mode, Fig. S6a. The TDC^{2-} ligands all adopt a (k^1-k^1-μ_2)-(k^1-k^1-μ_2)-μ_4 coordination mode, Fig. S6b. The Ac^- anion was produced by the decomposition of DMA solvent during the reaction.[21] It adopts a (k^2-k^2)-μ_3 coordination mode connecting three Mg^{2+} ions by chelating to Mg2 and linking to two Mg1 in both sides to form a [Mg_3(Ac)] unit, Fig. 4a.

Along the *c* axis, the Ac^- anions together with TDC^{2-} ligands connect the Mg1 and Mg2 ions to form a chain-like SBU characteristic of Mg1-Mg2-Mg1-Mg2 array, Fig. 4b. Each chain is interlinked to other four chains by TDC^{2-} ligands along the *a* and *b* axes. As a result, a 3D anionic framework is formed with large tunnels along the *c* axis in which the $[(Me)_2NH_2]^+$ cations, the free DMA molecules and H_2O molecules are located, Fig. 4c. Note that the structure of **3** is iso-structural with a Mn-based CP, namely $(Me_2NH_2)[(Mg_2(TDC)_2(Ac)]$.[22] The coordination mode of Ac^- anion in **3** can also be found in other compounds.[23] Taking the [Mg_3Ac] unit as a 4-connected node and TDC^{2-} ligand as a bridging linker, the framework of **3** could be simplified to a 4-connected uni-nodal net with a **crb** topology, Fig. 4d, and the Schläfli symbol is {4; 6^5}.

$[Mg_2(TDC)_2(DMF)_2(EtOH)(H_2O)_2]\cdot DMF$ (4). Compound **4** crystallizes in the noncentrosymmetric *Cm* space group featuring a 2D layered structure, Fig. 5. The asymmetric unit contains half of the formula unit including two halves of Mg^{2+} ions (each located in an inversion center), one TDC^{2-} ligand, one terminal coordinated DMF molecule, half of free DMF molecule, half of terminal EtOH molecule, half of terminal coordinated H_2O molecule and half of μ_2-coordinated H_2O molecule; the free DMF molecule and the terminal EtOH molecule are positional disordered by a mirror, and the O atom of the two halves unique H_2O molecules are located in a mirror.

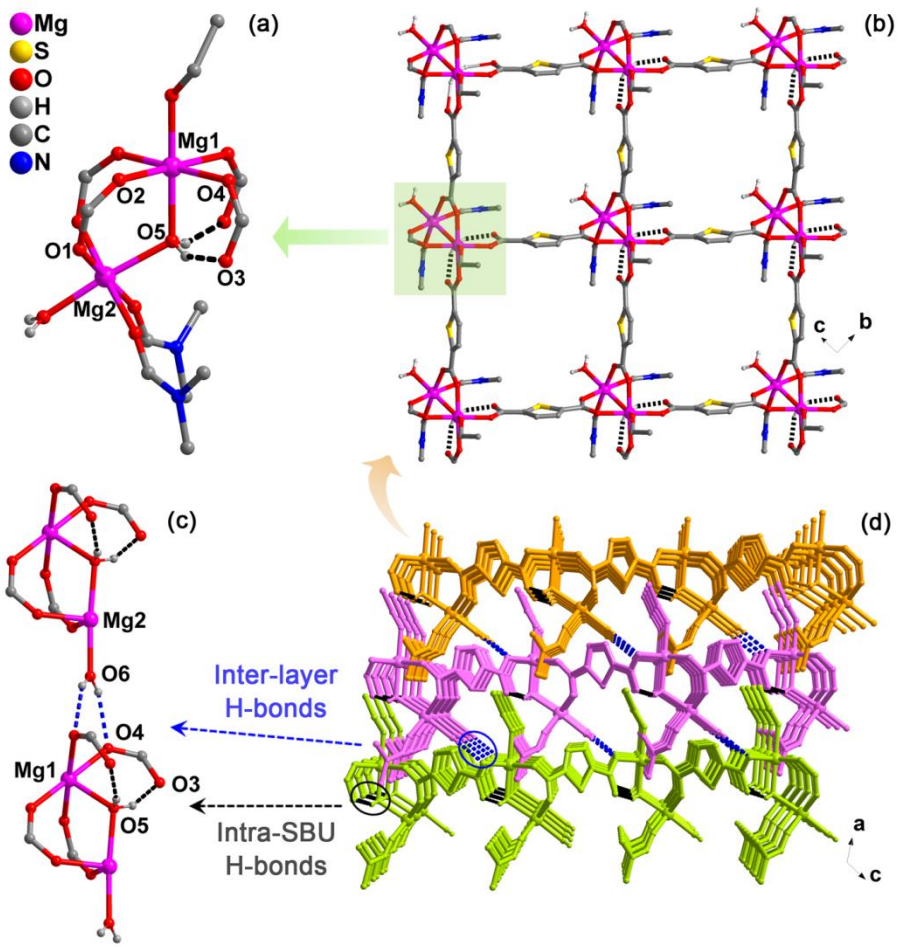

Fig. 5 (a) The bi-nuclear [$Mg_2(COO)_4(\mu_2$-$H_2O)$] SBU in **4**. (b) A single layer of **4**. (c) View of the 3D supramolecular structure of **4** with the three layers in different colors highlighting the "head to tail" packing mode of adjacent layers. (d) The intra-SBU and inter-layer H-bonding interactions between two SBUs from adjacent layers in **4**.

Both of Mg^{2+} centers adopt an octahedral geometry, Fig. S2d. Mg1 is occupied by four TDC^{2-} ligands in the equatorial plane, one EtOH molecule and one μ_2-H_2O molecule in the apical positions. Whereas Mg2 is coordinated by two TDC^{2-} ligands, two DMF molecules in the equatorial plane, one terminal and one μ_2-H_2O molecules in the apical positions, Fig. S7a. The TDC^{2-} ligand presents a common (k^1-k^1-μ_2)-(k^1-μ_1)-μ_3 mode with one carboxylic oxygen atom uncoordinated, Fig. S7b.

The Mg1 and Mg2 are connected by four TDC^{2-} ligands and one μ_2-H_2O to form a 4-connected bi-nuclear unit (Fig. 5a) which is quite different from the familiar paddle-wheel type $Zn(COO)_4$ unit in MOF-5.[24] In the unit, two carboxylate groups (O1, O2) of two TDC^{2-} ligands link Mg1 and Mg2 in a bi-bridge mode, while the other two carboxylate groups in another two ligands only bind to Mg1 (each with O4) in a mono-dentate mode with the uncoordinated O3 atoms forming strong H-bonds (O5-H5···O3 = 2.604(3) Å, ∠O5-H5-O3 = 153.2 °) with the μ_2-H_2O molecule. While the left coordination sites of two Mg^{2+} ions of the unit are occupied by solvent molecules (with EtOH molecule binding to Mg1, and H_2O and DMF molecules binding to Mg2, respectively). This dimmer can be viewed as the secondary building unit (SBU) of **4**. In the *bc* plane, each SBU is interlinked to another four ones by TDC^{2-} ligand to form a layer with rhombic grids, Fig. 5b and Fig. S8. Then, upon the H-bonding interactions among the terminal H_2O (O6) molecules in one layer and the carboxylate oxygen (O4) atoms in the other layer (O6-H6···O4 = 2.797(4) Å, ∠O6-H6-O4 = 145.3 °, Fig. 5c), these layers accumulate in the same direction, that is, in a "head to tail" fashion, to give rise to a 3D supramolecular structure, Fig. 5d. The solvent molecules are located in the spaces between and within layers, Fig. S10.

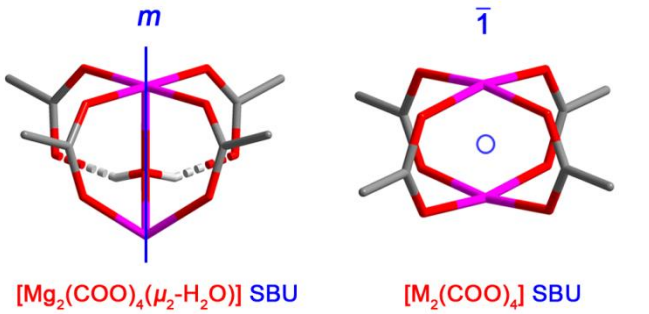

Fig. 6 The SBU of **4** in this work and the typical "paddle-wheel" type SBU in reported structures.[25]

Generally, to ensure a layered structure without an inversion center, two conditions must be satisfied including the NCS nature of a single layer and packing of these layers in a way without an inversion center.[2e] Lin et al. proved that for rhombic grids, the noncentrosymmetric metal coordinating centers could guarantee the NCS nature of the grids.[2e] Thrillingly, the μ_2-H_2O-containing SBU in **4** has a C_{2v} symmetry which absolutely rejects an inversion center. Accordingly, each layer of **4** is unsymmetrical. In comparison, the typical "paddle-wheel" shape $[M_2(COO)_4]$ SBU usually has a higher symmetry with an inversion center,[25] Fig. 6.

With a translation operation along the *c* axis, these layers accumulate to give the NCS structure of **4**.

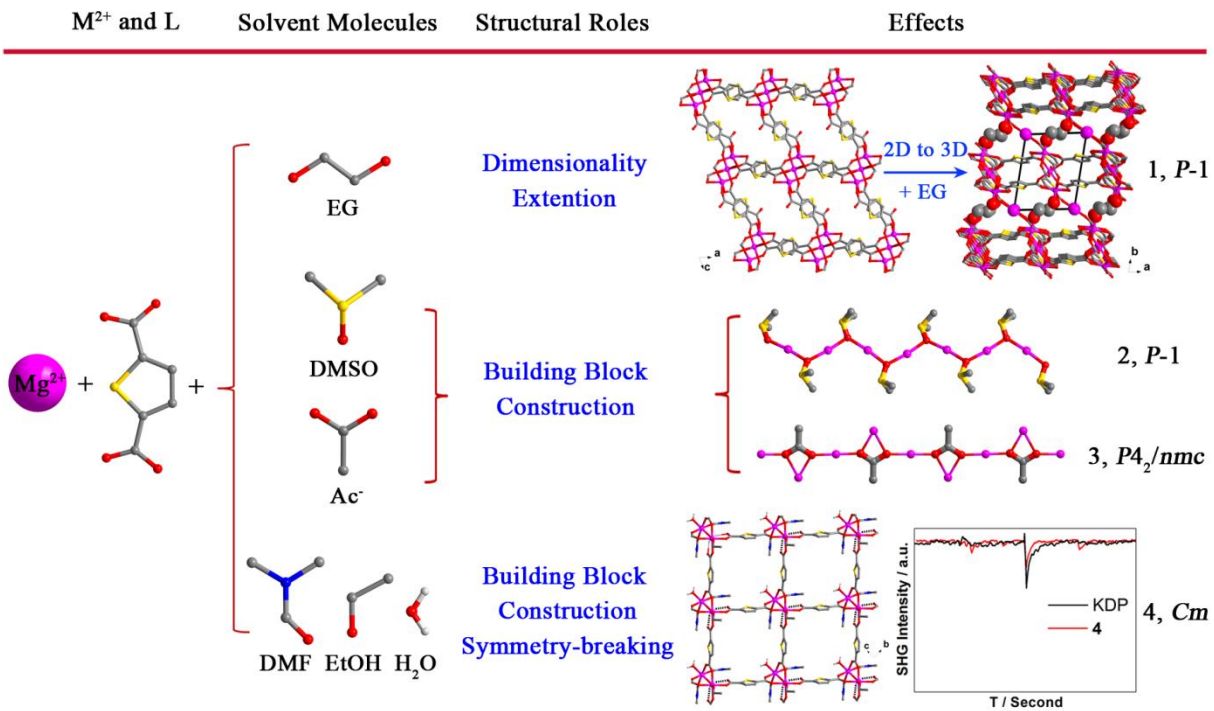

Scheme 1 Multi-roles of the solvent molecules in the construction of structures **1**-**4**. The data in the lower right corner: Oscilloscope traces of SHG signals of compound **4** and KDP (marker) in the particle size of 210–300 μm.

We presume the reasons why these layers prefer this packing mode as follows: i). the steric hindrance stemming from coordinated solvent molecules (DMF and H_2O in one side and ethanol in the other) is quite different in both sides of the layer which makes their packing prefer a "head to tail" fashion to maximally fill the void space within each layer, Fig. S10. There are reported layered structures with noncentrosymmetric layers featuring similar rhombic grids as that in **4**, but these layers have similar steric hindrance in both sides thus a "head to head" packing mode upon an inversion center results in centrosymmetric structures.[26] ii). this packing mode also facilitates the formation of inter-layer H-bonding interactions to further stabilize the whole structure. In a word, the multiple coordinated solvent molecules play vital roles in the symmetry-breaking process of forming **4**.

In the titled structures, Mg^{2+} ions all adopt the characteristic octahedral geometry, Fig. S2. The $Mg\text{-}O_{Carboxylate}$ bond distances of four structures varies from 1.995(2) to 2.182(2) Å for **1**, 2.020(3) to 2.063(3) Å for **2**, 2.0227(10) to 2.081(1) Å for **3** and 2.044(3) to 2.139(3) Å for **4**, all of which fall in the normal range of literature vales.[3b] The outstanding feature of these structures is that the coordinated solvent molecules as important structural components promote formation of the diverse structures, as summarized in Scheme 1.

PXRD patterns and thermal stability analyses

The phase purity of compounds **1-4** was confirmed by PXRD characterizations (Fig. 7a) and elemental analyses. Thermogravimetric analyses (TGA) were performed on the pure powder samples of **1-4** from 30 to 650 ℃, Fig. 7b. The multi-step weight losses of **1** from room temperature to 385 ℃ corresponded to the losses of free and terminal coordinated EG molecules and those as bridging ligands (about 32.6%, calc. 32.4%). **2** was stable up to 300 ℃; the sharp weight loss from 300 to 400 ℃ corresponded to the release of μ_2-DMSO molecules (about 28.7%, calc. 28.6%) which necessarily brought about the collapse of the framework. The open framework of **3** began to release free DMA molecules at room temperature followed by the escape of CH_3COOH molecules from the major framework, which inevitably caused the decomposition of the whole structure. In the temperature range of 90 ℃ to 390 ℃, **4** orderly released terminal EtOH molecules, terminal H_2O molecules, and free and terminal DMF molecules (weight loss: 43.1%, calc. 43.6%). All the four complexes are unstable at ambient conditions probably because of the strong interaction between Mg^{2+} ions in the frameworks with water molecules in the air which may cause the collapse of the framework.

Optical properties

Photoluminescence (PL) properties of compounds **1-3** in the solid state were investigated at room temperature. Crystals of **3** emits bright green light centred at 475 nm (monitored at λ_{ex} = 415 nm), Fig. 8, which is near the white light section convinced by the CIE chromaticity diagram, Fig. S11.[4f] While **1** and **2** show relatively weak emission with peaks centred at 480 and

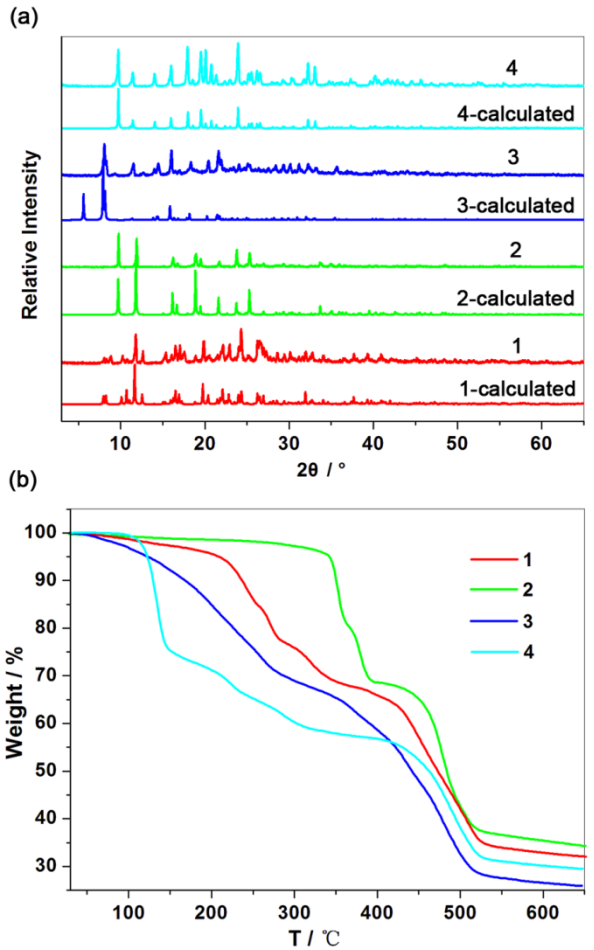

Fig. 7 The PXRD patterns (a) and TGA curves (b) of **1-4**.

455 nm (λ_{ex} = 407 nm and 375 nm), respectively, Fig. 8a. Monitored at 300 nm excitation wavelength, the free H_2TDC ligand features a blue light emission with a narrow peak centred at 350 nm, and the emission can be attributed to the $\pi^* \rightarrow n$ transition within the ligand.[27] Compared with the emission spectra of H_2TDC ligand, a bathochromic shift of the luminescence is observed in the three compounds. Considering the electronic configuration of Mg^{2+}, the red-shift of emission may be derived from the increase of the ligand conjugation degree after coordinated with Mg^{2+} ions.[2b, 28]

Nonlinear optics (NLO) possess practical importance due to its applications in telecommunications, optical storage, information processing and so on.[29] One of the most common NLO behaviours is second-harmonic generation (SHG), in which a NLO material can amplify light signal by doubling the frequency.[2e] NLO properties require that the crystal structure belongs to the noncentrosymmetric space group.[30] Considering the acentric nature of the structure of **4**, the SHG properties of **4** was investigated on the powder samples by using the Kurtz–Perry method.[11] An approximate estimation was carried out on a pulsed Q-switched Nd:YAG laser at a wavelength of 1064 nm. The intensity of the green light (λ = 532 nm) produced by the

crystal powder of **4** is about 0.5 times that of a KDP (KH_2PO_4) marker, which is sound among other SHG materials, Fig. S12.

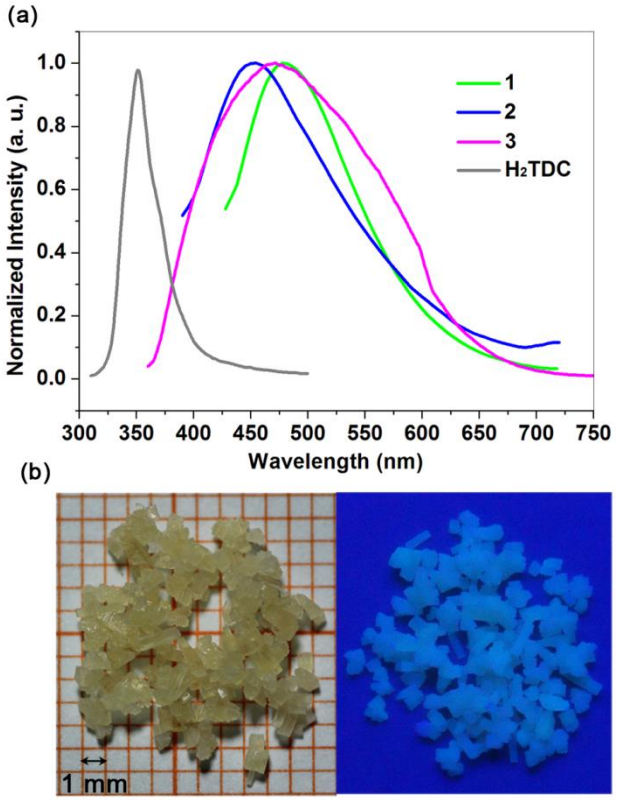

Fig. 8 (a) Solid-state PL emission spectra of **1-3** and H_2TDC ligand at room temperature. (b) Photographs of the crystals and its luminescence under 365 nm UV light of **3**.

Conclusions

Four Mg-TDC CPs were solvothermally synthesized in different mixed solvents. Compounds **1-3** feature a 3D infinite framework while **4** has a 2D layered structure. The solvent molecules play vital roles in the formation of these structures by contributing to the extension of the structural dimensionality in **1** and fabrication of the chain-like SBUs in **2** and **3**. Moreover, for the layered structure of **4**, the structural origin of its noncentrosymmetric nature has been discussed in detail, which shows that the mixed coordinated solvent molecules may play a crucial role in the formation of noncentrosymmetric structure. Photoluminescence emissions and SHG response were investigated for the selected titled compounds which showed that compound **3** displayed bright green light emission and compound **4** displayed sound SHG response. The isolation of these compounds may supply important instructions on the synthesis of Mg-based CPs which is so sensitive to solvent systems that their structures are hardly predictable.

Acknowledgements

This work was granted by the NNSF of China (nos. 21221001 and 21403233), and the 973 program (no. 2012CB821702).

Notes and references

[a] State Key Laboratory of Structural Chemistry, Fujian Institute of Research on the Structure of Matter, Chinese Academy of Sciences, Fuzhou, Fujian, 350002, P.R. China
[b] University of Chinese Academy of Sciences, Beijing, 100049, P.R. China
* E-mail: xyhuang@fjirsm.ac.cn; Fax: (+86)591–83793727

† Electronic Supplementary Information (ESI) available: A list of additional reactions, TG-MS figure, more structural figures, CIE chromaticity diagram, SHG figure and IR spectra for compounds **1-4**. CCDC reference numbers 1032293 (**1**), 1032294 (**2**), 1032295 (**3**) and 1032296 (**4**). See DOI: 10.1039/b000000x/

1 G. Ferey, *Chem. Soc. Rev.*, 2008, **37**, 191-214.
2 (*a*) A. Corma, H. Garcia and F. X. L. Xamena, *Chem. Rev.*, 2010, **110**, 4606-4655; (*b*) Y. J. Cui, Y. F. Yue, G. D. Qian and B. L. Chen, *Chem. Rev.*, 2012, **112**, 1126-1162; (*c*) L. E. Kreno, K. Leong, O. K. Farha, M. Allendorf, R. P. Van Duyne and J. T. Hupp, *Chem. Rev.*, 2012, **112**, 1105-1125; (*d*) M. P. Suh, H. J. Park, T. K. Prasad and D. W. Lim, *Chem. Rev.*, 2012, **112**, 782-835; (*e*) C. Wang, T. Zhang and W. B. Lin, *Chem. Rev.*, 2012, **112**, 1084-1104; (*f*) R. C. Huxford, J. Della Rocca and W. B. Lin, *Curr. Opin. Chem. Biol.*, 2010, **14**, 262-268.
3 (*a*) K. M. Fromm, *Coord. Chem. Rev.*, 2008, **252**, 856-885; (*b*) D. Banerjee and J. B. Parise, *Cryst. Growth Des.*, 2011, **11**, 4704-4720.
4 (*a*) S. R. Caskey, A. G. Wong-Foy and A. J. Matzger, *J. Am. Chem. Soc.*, 2008, **130**, 10870-10871; (*b*) D. Britt, H. Furukawa, B. Wang, T. G. Glover and O. M. Yaghi, *Proc. Natl. Acad. Sci. U. S. A.*, 2009, **106**, 20637-20640; (*c*) M. Dincă and J. R. Long, *J. Am. Chem. Soc.*, 2005, **127**, 9376-9377; (*d*) J. A. Rood, W. C. Boggess, B. C. Noll and K. W. Henderson, *J. Am. Chem. Soc.*, 2007, **129**, 13675-13682; (*e*) A. E. Platero-Prats, V. A. de la Pena-O'Shea, D. M. Proserpio, N. Snejko, E. Gutierrez-Puebla and A. Monge, *J. Am. Chem. Soc.*, 2012, **134**, 4762-4771; (*f*) Z.-F. Wu, B. Tan, J.-Y. Wang, C.-F. Du, Z.-H. Deng and X.-Y. Huang, *Chem. Commun.*, 2015, **51**, 157-160; (*g*) Z. F. Wu, B. Tan, M. L. Feng, A. J. Lan and X. Y. Huang, *J. Mater. Chem. A*, 2014, **2**, 6426-6431.
5 M. Mazaj, T. B. Celic, G. Mali, M. Rangus, V. Kaucic and N. Z. Logar, *Cryst. Growth Des.*, 2013, **13**, 3825-3834.
6 O. M. Yaghi, M. Eddaoudi, J. Kim, N. Rosi, D. Vodak, J. Wachter and M. O'Keeffe, *Science*, 2002, **295**, 469-472.
7 (*a*) D. Banerjee, J. Finkelstein, A. Smirnov, P. M. Forster, L. A. Borkowski, S. J. Teat and J. B. Parise, *Cryst. Growth Des.*, 2011, **11**, 2572-2579; (*b*) S. C. Chen, Z. H. Zhang, K. L. Huang, Q. Chen, M. Y. He, A. J. Cui, C. Li, Q. Liu and M. Du, *Cryst. Growth Des.*, 2008, **8**, 3437-3445.
8 V. R. Pedireddi and S. Varughese, *Inorg. Chem.*, 2004, **43**, 450-457.
9 (*a*) J. D. Lin, X. F. Long, P. Lin and S. W. Du, *Cryst. Growth Des.*, 2010, **10**, 146-157; (*b*) Z. J. Lin, Z. Yang, T. F. Liu, Y. B. Huang and R. Cao, *Inorg. Chem.*, 2012, **51**, 1813-1820.
10 T. Liu, D. Luo, D. Xu, H. Zeng and Z. Lin, *Inorg. Chem. Commun.*, 2013, **29**, 110-113.
11 S. K. Kurtz and T. T. Perry, *J. Appl. Phys.*, 1968, **39**, 3798-3813.
12 G. M. Sheldrick, *SHELX 97, Program for Crystal Structure Solution and Refinement, University of Gättingen: Germany*, 1997.

13 (*a*) P. Vandersluis and A. L. Spek, *Acta Crystallogr., Sect. A*, 1990, **46**, 194-201; (*b*) A. L. Spek, *J. Appl. Crystallogr.*, 2003, **36**, 7-13.
14 A. Rossin, A. Ienco, F. Costantino, T. Montini, B. Di Credico, M. Caporali, L. Gonsalvi, P. Fornasiero and M. Peruzzini, *Cryst. Growth Des.*, 2008, **8**, 3302-3308.
15 Q. R. Fang, X. Shi, M. H. Xin, G. Wu, G. Tian, G. S. Zhu, Y. F. Li, L. Ye, C. L. Wang, Z. D. Zhang, L. L. Tang and S. L. Qiu, *Chem. J. Chin. Univ.*, 2003, **24**, 980-982.
16 H. L. Gao, L. Yi, B. Ding, H. S. Wang, P. Cheng, D. Z. Liao and S. P. Yan, *Inorg. Chem.*, 2006, **45**, 481-483.
17 X. C. Yi, L. Yan and E. Q. Gao, *Acta Crystallogr., Sect. E: Struct. Rep. Online*, 2010, **66**, M1554-U1695.
18 Q. R. Fang, G. S. Zhu, X. Shi, M. H. Xin, G. Wu, G. Tian, L. Ye, C. L. Wang, Z. D. Zhang and S. L. Qiu, *Chem. J. Chin. Univ.*, 2003, **24**, 776-778.
19 S. J. Wang, S. S. Xiong, L. X. Song and Z. Y. Wang, *CrystEngComm*, 2009, **11**, 896-901.
20 J. D. Lin, S. T. Wu, Z. H. Li and S. W. Du, *CrystEngComm*, 2010, **12**, 4252-4262.
21 D. F. Sun, Y. X. Ke, D. J. Collins, G. A. Lorigan and H. C. Zhou, *Inorg. Chem.*, 2007, **46**, 2725-2734.
22 Y. X. Tan, Y. P. He, Y. Zhang, Y. J. Zheng and J. Zhang, *CrystEngComm*, 2013, **15**, 6009-6014.
23 (*a*) W. X. Chen, Y. P. Ren, L. S. Long, R. B. Huang and L. S. Zheng, *CrystEngComm*, 2009, **11**, 1522-1525; (*b*) Y. W. Li, J. P. Zhao, L. F. Wang and X. H. Bu, *CrystEngComm*, 2011, **13**, 6002-6006; (*c*) J. Zhou, S. H. Yan, D. Q. Yuan, X. J. Zheng, L. C. Li and L. P. Jin, *CrystEngComm*, 2009, **11**, 2640-2649.
24 O. M. Yaghi, H. Li, M. Eddaoudi and M. O'Keeffe, *Nature*, 1999, **402**, 276-279.
25 S. S. Y. Chui, S. M. F. Lo, J. P. H. Charmant, A. G. Orpen and I. D. Williams, *Science*, 1999, **283**, 1148-1150.
26 (*a*) M. Lv and S. W. Ng, *Acta Crystallogr., Sect. E: Struct. Rep. Online*, 2007, **63**, M3136-U2489; (*b*) S. Y. Yang, L. S. Long, R. B. Huang, L. S. Zheng and S. W. Ng, *Acta Crystallogr., Sect. E: Struct. Rep. Online*, 2005, **61**, M1671-M1673; (*c*) Y. B. Lou, J. J. Wang, Y. H. Tao, J. X. Chen, A. Mishima and M. Ohba, *Dalton Trans.*, 2014, **43**, 8508-8514.
27 P. J. Calderone, D. Banerjee, A. C. Santulli, S. S. Wong and J. B. Parise, *Inorg. Chim. Acta*, 2011, **378**, 109-114.
28 X. Li, X. W. Wang and Y. H. Zhang, *Inorg. Chem. Commun.*, 2008, **11**, 832-834.
29 (*a*) K. Jain and G. W. Pratt, *Appl. Phys. Lett.*, 1976, **28**, 719-721; (*b*) *Nonlinear Optical properties of Organic Molecules and Crystals*, **vol. 1**, ed. J. Zyss and D. S. Chemla, Academic Press, New York, 1989, p. 23; (*c*) D. A. Keszler, *Current Opinion in Solid State & Materials Science*, 1999, **4**, 155-162.
30 Nye, J. F. *Physical properties of crystals: their representation by tensors and matrices*; Clarendon: Oxford, 1985.

Table of Contents

Four Mg-TDC CPs have been isolated solvothermally in which the solvent molecules play vital roles in constructing the diverse structures.